

Toward more realistic NEGF simulations of vertically stacked multiple SiNW FETs

Hong-Hyun Park^{1*}, Woosung Choi¹,
 Mohammad Ali Pourghaderi², Jongchol Kim², Uihui Kwon², and Dae Sin Kim²
¹Device Laboratory, Samsung Semiconductor Inc., San Jose, California, USA
²Semiconductor R&D Center, Samsung Electronics, Hwasung-si, Gyeonggi-do, Korea
 *e-mail: honghyun.p@samsung.com

Abstract—We present quantum transport simulation results of vertically stacked multiple silicon nanowire (SiNW) FETs based on the non-equilibrium Green’s function (NEGF) method. In order to consider more realistic device conditions such as complex geometry of the multi-channel FETs and various carrier scattering processes, we improved physical models and numerical techniques for the NEGF simulations.

Keywords—quantum transport, non-equilibrium Green’s function (NEGF), multiple nanowire FET

I. INTRODUCTION

Nowadays the FinFET technology is the most advanced node for commercial logic device fabrications. Its success was enabled mainly by the larger effective channel width and stronger gate controllability than previously used planar FETs. As long as we use the concept of field-effect transistor, a key technology requirement to boost the device performances will be to achieve better gate controllability. Hence, gate all-around (GAA) FETs are being studied as an ultimate structure for future logic devices.

As a transition technology to GAA FETs, vertically stacked multiple nanowire structure is considered as one of the strong candidates since the fabrication processes have many parts in common with those of FinFETs [1]. Fig. 1 shows an example of dual-channel SiNW FET, where the channels are enclosed by a gate contact as a whole different from GAA FETs. Since there is little data from actual measurements of multiple SiNW FETs and there seem to be some quantum effects which should be addressed carefully, we decided to rely on quantum transport simulations for the performance estimations of the devices. We especially employed the NEGF approach because of its rigorous and general theoretical basis.

Usually, quantum transport models have been used to simulate relatively simple device structures such as single nanowire FETs where source/drain contacts are modelled just as extensions of the channel region. In order to study various effects of complex geometrical and process conditions of multiple SiNW FETs on the device performances, we have improved our in-house NEGF solver in terms of model flexibility and computational efficiency.

In this paper we explain our simulation models and demonstrate some of our simulations of dual-channel SiNW nFETs.

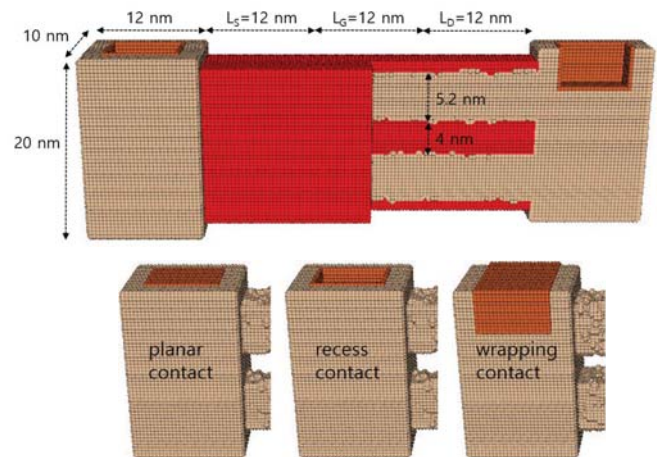


Fig. 1. Simulated dual-channel SiNW nFET. Silicon, oxide, and contact metal regions are represented in ivory, red, and orange colors, respectively. This particular structure has two SiNWs as its channels and bulky epitaxial regions for source and drain. The channels are doped with p-type ($3E18/cm^3$) and the source/drain regions are doped with n-type ($2E20/cm^3$). The effective thickness of the gate oxide layer is about 0.85 nm. Planar-, recess-, and wrapping-type contacts are tested.

II. SIMULATION METHOD

An example structure of a dual-channel SiNW nFET is shown in Fig. 1. In our quantum transport simulations the NEGF solver covers the silicon region for carrier transport while the Poisson solver covers the whole region for electrostatic potential. We implemented several existing simulation models in order to consider major physical effects such as the bandstructure and scattering of carriers. We also developed new models to simulate realistic and complex simulation domains. More explanations are followed.

A. Numerical methods

Most of an NEGF simulation is about the calculations of various Green’s functions. For example, the retarded Green’s function is obtained as follow:

$$\mathbf{G}(E) = [\mathbf{E}\mathbf{I} - \mathbf{H} - \Sigma]^{-1}$$

In the following, the numerical methods that we improved for efficient NEGF simulations of arbitrary-shaped structures are explained.

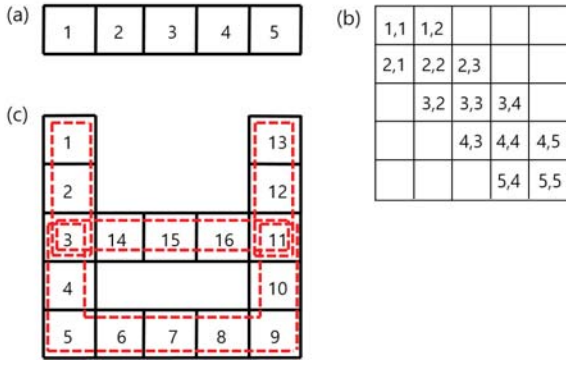


Fig. 2. (a) Schematic of the blocks (squares with block index) of a linear-shaped simulation domain. (b) Block tri-diagonal matrix obtained from the linear-shaped simulation domain. (c) Schematic of the blocks of a complex-shaped simulation domain. The domain can be decomposed into the four sections specified in red for the extended RGF technique.

1) In the case that \mathbf{G}^{-1} matrix has a block tri-diagonal form the recursive Green's function (RGF) technique can be applied for better numerical efficiency than inverting the whole matrix at once [2, 3]. The ideal block tri-diagonal form is obtained when the range of inter-atomic interactions is short and the shape of a simulation domain is linear like a single nanowire FET. If the shape of a simulation domain is not linear, then the corresponding \mathbf{G}^{-1} deviates from the ideal block tri-diagonal form and the efficiency of the conventional RGF method becomes worse accordingly. In this case numerical reordering techniques can be applied to transform \mathbf{G}^{-1} to more ideal block tri-diagonal form but additional overheads are involved and the physical meaning of intermediate solutions during the RGF computation may become unclear. In this work we extend the conventional RGF technique to be applicable to arbitrary-shaped devices with the same or similar numerical efficiency as the conventional RGF technique. The key idea is to decompose a complex simulation domain into multiple linear sections as shown in Fig. 2. The detailed procedure of the extended RGF technique is beyond the scope of this paper. Except for a matrix inversion of the connecting blocks between the sections, the conventional RGF technique can be applied to each section independently.

2) The mode-space approach (MS) is widely used to improve the speed of NEGF simulations significantly [4]. Originally, the method is available for linear-shaped devices only because the calculation of the eigenvectors used for MS transformation assumes that each block has periodicity along the transport direction. In our simulations, however, the blocks can have arbitrary shapes and each block may not have a unique transport direction. So, we introduce pseudo-periodicity for each block so that the MS approach is still available for the NEGF simulations of arbitrary-shaped devices.

B. Simulation Models

Simulation models determine the quality of the simulation results. Some of the simulation models used in this study are explained in the following.

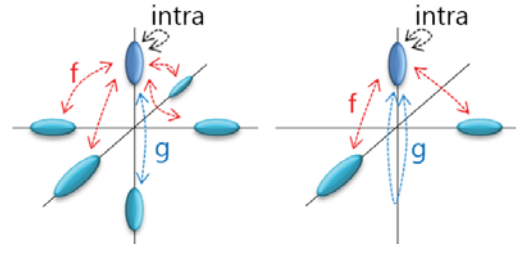


Fig. 3. (left) Six valleys of the conduction band of silicon. Intra- and inter-valley electron-phonon scattering processes at the valley colored blue. (right) Equivalent scattering processes in the case of a simulation with three-valley model, where g-type processes are treated like intra-valley processes and the scattering rates for f-type processes must be doubled.

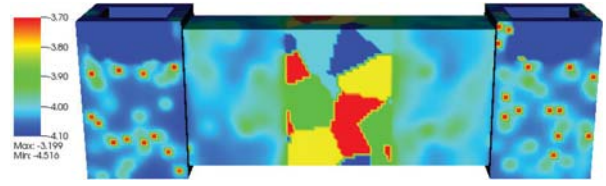


Fig. 4. Electrostatic potential profile on the surface of the simulated dual-channel SiNW nFET. The range of the colormap is narrowed to show the distribution of the gate workfunction clearly.

1) The bandstructure of the conduction band of silicon is modelled by the effective-mass approximation (EMA) with nonparabolicity corrections [5, 6]. For the sake of numerical efficiency only three valleys are considered in the simulations as shown in Fig. 3. The model parameters for each valley are calibrated against tight-binding simulation results [7] to take into account the effects of quantum confinement and strain/stress more accurately.

2) Electron-phonon scattering is modelled based on the deformation potential theory [8] which can capture intra- and inter-valley scattering processes as shown in Fig. 3. To fit experimentally observed mobility decrease in the strong inversion regime, the deformation potential values are adjusted to be enhanced near the surface of the channel [9].

3) Atomistic doping model is used to consider the effects of dopant variation and impurity scattering explicitly in the NEGF simulations. Random and discrete point charges are generated from a given continuous doping profile according to Poisson statistics.

4) Surface roughness in the channels is generated according to given sets of amplitude and correlation length [4] as shown in Figs. 1 and 7. Different random seeds are applied to different channels.

5) To consider the variability effect due to the gate metal phenomenologically, it is assumed that the gate metal consists of grains with random sizes and workfunction values. In this model some parameters such as the distribution of the grain size and the distribution of workfunction values are necessary. Fig. 4 shows an example of workfunction distribution reflected to the electrostatic potential.

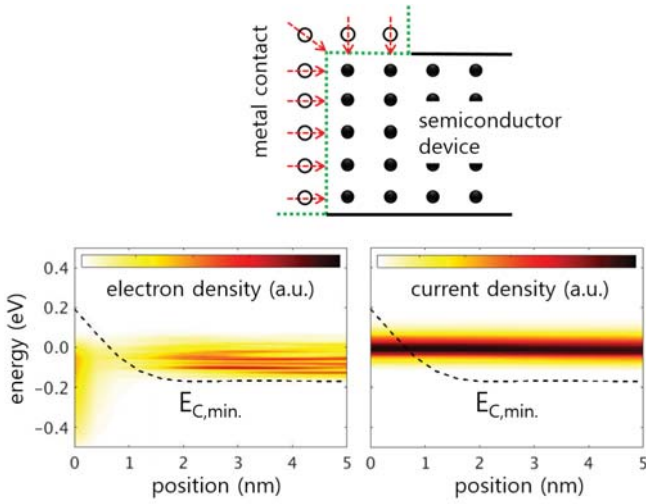


Fig. 5. (upper) Schematic of a metal-semiconductor contact. The arrows at contact atoms indicate the incident directions set to be normal to the contact interface. (lower) Electron and current density profiles in a semiconductor near a Schottky contact that is located at the origin in the figures.

6) Schottky contacts are attached on the source/drain epitaxial regions as shown in Fig. 1. Usually in quantum transport simulations, it is assumed that a contact is a semi-infinite extension of the contact part of the simulation domain [4, 10], which is not appropriate for realistic metal-semiconductor interfaces. So, in this work the contact model was improved more realistically by two modifications. Firstly, virtual metals are introduced for contacts. Each type of metal requires three parameters under EMA model, i.e. workfunction, band edge, and effective mass. The workfunction parameter is used to give desired Schottky barrier height when a Dirichlet boundary condition is applied to the contact and the other parameters are calibrated to give desired I-V characteristic or Schottky resistance. Secondly, the new contact model assumes that each of the contact atoms is an independent reservoir of carriers and does not interact with the other contact atoms. By this assumption different incident directions can be set for different contact atoms so the shape of a contact can be an arbitrary curved surface. Another advantage is that the calculation of the contact self-energy function is much faster than that of conventional contact models because the function can be evaluated independently for each atom. More graphical explanation of the Schottky contact model is shown in Fig. 5.

III. SIMULATION RESULTS

Although simulations of triple- or quad-channel SiNW FETs are possible, we only show the results of the dual-channel SiNW nFETs shown in Fig. 1. Please note that the simulated device structures and conditions are not optimized in terms of device performances. All the simulation results are obtained from self-consistent NEGF simulations with the models mentioned in the previous section unless special notes are made. A typical simulation time for each bias condition is about 2~3 hours with MPI parallelization using 80 CPUs.

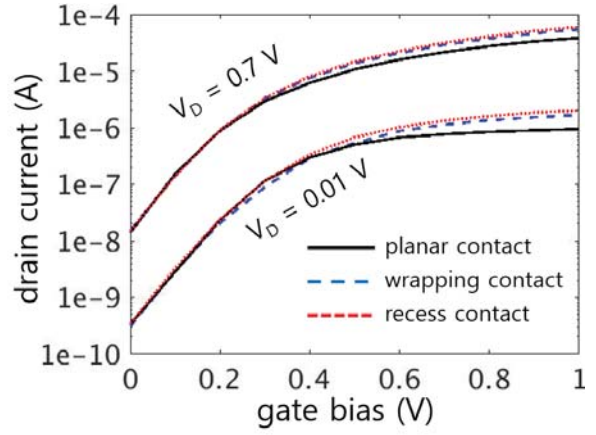


Fig. 6. I_D - V_G characteristic of the simulated dual-channel SiNW nFETs with three different shapes of Schottky contacts.

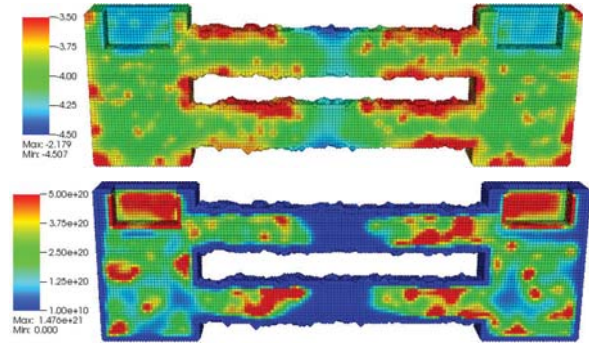
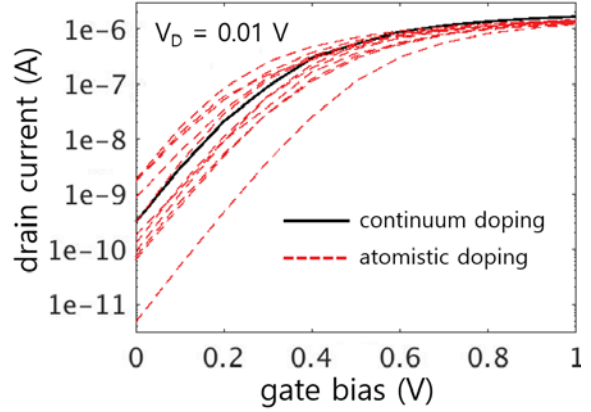


Fig. 7. (upper) Distribution of I_D - V_G curves from the simulated dual-channel SiNW nFETs with 11 different configurations of random dopants. (lower) Electric potential (V) and electron density ($1/\text{cm}^3$) profiles at $V_G = 0$ V and $V_D = 0.01$ V.

Fig. 6 shows the I_D - V_G characteristics of the simulated dual-channel SiNW nFETs with three different shapes of Schottky contacts as shown in Fig. 1. Here, in order to compare the effect of contact type on I-V characteristic clearly without the effect of fluctuation, we used a continuum doping model instead of atomistic and random dopants. The surface

roughness and random workfunction distribution do not result in significant fluctuation because their correlation lengths are relatively short. All the three FETs show similar subthreshold slope since they have the same electrostatic controllability over the channel region. In terms of the on-current level, however, the FETs with planar-type contacts show smaller values than those with the other contact types because of higher access resistance.

Fig. 7(upper) shows the distribution of I_D - V_G curves of the simulated dual-channel SiNW nFETs with recess-type contacts, where the large variation in the sub-threshold voltage results from the different configurations of atomistic random dopants. Also, the atomistic dopants result in the decrease in the on-current levels by the effect of impurity scattering which is missing in the case of the continuum doping model.

Fig. 7(lower) shows the electric potential and electron density profiles obtained as solutions of an off-state bias condition. The fluctuation in the profiles are mainly due to atomistic dopants. In the case with random dopants it is usually more difficult to reach the numerical convergence of the NEGF simulations than those with the continuum doping model. Hence, proper treatments of the simulation conditions and the convergence schemes are very critical for accurate results.

IV. CONCLUSION

In this paper, it was shown that various physical models and numerical techniques in our in-house NEGF solver are improved for more accurate, efficient, and flexible quantum transport simulations of semiconductor devices. The development enabled realistic simulations of complex-shaped devices like vertically stacked multiple nanowire FETs with the consideration of various physical effects like Schottky

resistance, electron-phonon scattering, atomistic dopants, surface roughness, random workfunction variation etc. Simulations of dual-channel SiNW nFETs were demonstrated and discussed briefly.

REFERENCES

- [1] B.-H. Lee, M.-H. Kang, D.-C. Ahn, J.-Y. Park, T. Bang, S.-B. Jeon, J. Hur, D. Lee, and Y.-K. Choi, "Vertically Integrated Multiple Nanowire Field Effect Transistor," *Nano Lett.* 15 (12), pp. 8056-8061, 2015.
- [2] R. Lake, G. Klimeck, R. C. Bowen, and D. Jovanovic, "Single and multiband modeling of quantum electron transport through layered semiconductor devices," *J. Appl. Phys.* 81 (12), pp. 7845-7869, 1997.
- [3] M. P. Anantram, M. S. Lundstrom, and D. E. Nikonov, "Modeling of Nanoscale Devices," *Proc. IEEE*, vol. 96, no. 9, pp. 1511-1550, 2008.
- [4] M. Luisier, "Quantum Transport Beyond the Effective Mass Approximation," ETH Zurich, 2007.
- [5] W. R. Frensley, "Boundary conditions for open quantum systems driven far from equilibrium," *Rev. Mod. Phys.*, vol. 62, no. 3, pp. 745-791, 1990.
- [6] E. O. Kane, "Band structure of indium antimonide," *J. Phys. Chem. Solids*, vol. 1, pp. 249-261, 1957.
- [7] J. C. Slater and G. F. Koster, "Simplified LCAO Method for the Periodic Potential Problem," *Phys. Rev.*, vol. 94, no. 6, pp. 1498-1524, June 1954.
- [8] S. Jin, Y. J. Park, and H. S. Min, "A three-dimensional simulation of quantum transport in silicon nanowire transistor in the presence of electron-phonon interactions," *J. Appl. Phys.*, vol. 99 (12), pp. 123719-123729, 2006.
- [9] T. Ohashi, T. Tanaka, T. Takahashi, S. Oda, and K. Uchida, "Experimental Study on Deformation potential (D_{ac}) in MOSFETs: Demonstration of Increased D_{ac} at MOS Interfaces and Its Impact on Electron Mobility," *IEEE J. Electron Devices Soc.*, vol. 4, pp. 278-285, 2016.
- [10] M. P. Lopez Sancho, J. M. Lopez Sancho, and J. Rubio, "Highly convergent schemes for the calculation of bulk and surface Green functions," *J. Phys. F: Met. Phys.* 15, pp. 851-858, 1985.